# CrystEngComm

Accepted Manuscript






ROYAL SOCIETY OF CHEMISTRY

www.rsc.org/crystengcomm

# Temperature-induced one-dimensional chiral Ag(I) linear chain and left-handed $2_1$ helix: DFT studies, luminescence and SHG response

Lin Cheng,[a,b,*] Jun Wang,[a,b] Qi Qi,[a] Xiuying Zhang,[a] Hai-Yan Yu,[a] Shaohua Gou[a,b*] and Lei Fang[a,b]

[a] Pharmaceutical Research Center, School of Chemistry and Chemical Engineering, Southeast University, Nanjing 211189, China

[b] Jiangsu Province Hi-Tech Key Laboratory for Bio-medical Research, Southeast University, Nanjing 211189, China

## Abstract

Two pairs of chiral coordination polymers, $\{\{Ag[(1R,2R)\text{-3-bcpb}]\}\cdot X\cdot H_2O\cdot CH_3OH\}_n$ [X = $NO_3$ (**1a**), $ClO_4$ (**1b**)] and $\{\{Ag[(1R,2R)\text{-3-bcpb}]\}\cdot X\cdot 3H_2O\}_n$ [X = $NO_3$ (**2a**), $ClO_4$ (**2b**)] (where (1*R*,2*R*)-3-bcpb = *N*,*N*'-((1*R*,2*R*)-cyclohexane-1,2-diyl)bis(*N*-(pyridin-3-ylmethyl)benzamide), have been synthesized with the same materials at 25 and 90 °C, respectively. **1a** and **1b** are 1D chiral linear chains, while **2a** and **2b** display left-handed $2_1$ helical chains with dual chiral components, including the congenital chiral carbon centres and the acquired chirality of the single-handed helices. **1a** and **1b** can be transformed to **2a** and **2b**, respectively, by heating; while the reverse operations failed. The structural difference of **1a** (**1b**) and **2a** (**2b**) may be attributed to the different configurations of the ligand, which are highly influenced by the reaction temperature and further theoretically explained by DFT calculations. The luminescent studies revealed interesting emission bands. Circular dichroism spectra and second-harmonic generation efficiency measurements of the products have been investigated as well, which indicate their potential applications in chiral and nonlinear optical areas.

* Corresponding author: lcheng@seu.edu.cn, sgou@seu.edu.cn. Tel: +86-025-83272381; Fax: +86-025-83272381

## Introduction

In the past few decades, chiral coordination polymers (CCPs) have been extensively studied due to their intriguing variety of architectures and topologies, as well as their potential applications in asymmetric catalysis, enantioselective separations, biomimetic chemistry, nonlinear optical materials, ferroelectric and magnetic materials.[1,2] Such CCPs can usually be achieved from:[3,4] (i) chiral organic linkers, which are used to connect adjacent metal ions; (ii) chiral auxiliary agents, that does not directly participate in the formation of the framework backbone but forces the framework to adopt a specific chiral topology; (iii) achiral reagents by spontaneous resolution *via* symmetry breaking crystallization. The first approach is straightforward and the application of chiral bridging ligands can ensure the chirality of the resultant network structures,[3a] while the latter two methods are both determined by the asymmetric crystallization of achiral precursors, but they depend on the controllable and random symmetry breaking, respectively.[4d] Consequently, the chirality of these homochiral coordination polymers originates from either the inherent and congenital chirality of the raw materials or the formed and acquired chirality *via* the coordination interactions with the generation of chiral centers, optically pure isomer, single-handed helices and/or chiral topologies. CCPs with dual chiral components (congenital and acquired chirality) not only have special and interesting structural features, but also have many potential applications. For instance, such polymers may offer multiple active sites for concerted catalysis, multifunctional catalysis or selective catalysis in an asymmetric catalytic system. Until now, large quantities of CCPs with congenital chirality or acquired chirality have been reported. Nevertheless, only a few CCPs with dual chiral components are known, and the structural information for potential applications is limited.[5-9] Therefore, we have paid our interest to the synthesis of CCPs with dual chiral components by designing a series of (1*R*,2*R*)-$N^1$,$N^2$-bis(pyridinylmethyl)cyclohexane-1,2-diamine derivatives (Scheme 1a),[9] which have following features: (1) the 1,2-diaminocyclohexyl skeleton has congenital chirality with two inherent chiral carbon atoms; (2) the two secondary amines are easy to chelate one metal ion, leading to the formation of acquired chiral nitrogen atoms; (3) C-N bonds are

more flexible than C=N bonds and may rotate freely, which improves the helix elements of generated CCPs.

On the other hand, how to rationally design and synthesize coordination polymers (CPs) with desired properties has been a long term challenge because their assembly process is highly influenced by many factors,[10,11] in which reaction temperature has been verified as an important role in the construction of the overall architectures of CPs, mainly because of its influence on the coordination ability and conformations of organic ligands, as well as the coordination number and coordination geometries of the metal centers.[12,13] Generally, the thermodynamically favored conformer, associated with a large activation barrier, can be obtained at high temperature, while low temperature favors the kinetic conformer because the thermal energy relies on the temperature proportionally.[14] Meanwhile, one-dimensional (1D) CPs are the simplest topological type of coordination array, and the relative simplicity of their structures and the ease of formation by self-assembly make them become ideal research targets in the crystal engineering of CPs.[15] In addition, there are a lot of temperature-controlled CPs with different dimensions in the references, but only several examples of temperature-induced 1D CPs with different topologies, such as zigzag chain, helical chain, linear chain, and so on, have been published.[16] It's worth noting that, until now, no theoretical calculations (such as DFT) have been carried out to understand the nature and role of temperature in the final structural formation of 1D CPs.

Herein, we design a new chiral ligand-*N*,*N*'-((1*R*,2*R*)-cyclohexane-1,2-diyl)bis(*N*-(pyridin-3-ylmethyl)benzamide) ((1*R*,2*R*)-3-bcpb), as one member of chiral diamine derivatives, which has the following unique characteristics, compared with the chiral diamine ligands that we have reported (Scheme 1c):[9] (i) as a part of acylamide, the nitrogen atoms don't participate in the coordination interaction with metal ions, and the whole molecule becomes a simple V-shaped bidentate ligand, which helps to the construction of 1D CCPs, including helical chains; (ii) it not only has *cis*- and *trans*-isomers based on the N-positions of the two pyridyl rings, like that of the (1*R*,2*R*)-3-bpcd ligand (Scheme 1b, 1c and S1), but also has other isomers based on the relationship between the phenyl and pyridyl rings of the two sides (Scheme 2), consequently the configuration diversification of the ligand

occurs, which helps to understand the effect of temperature on the configurations of the ligand and the structures of the resultant 1D CCPs. Meanwhile, because of the easy availability and flexibility, potential physical and chemical functions, as well as the diverse coordination numbers and geometries of Ag(I) ion,[17] here we continue to select Ag(I) as metal nodes to construct CCPs. As expected, two pairs of CCPs, $\{\{Ag[(1R,2R)\text{-3-bcpb}]\}\cdot X\cdot H_2O\cdot CH_3OH\}_n$ [X = $NO_3$ (**1a**), $ClO_4$ (**1b**)] and $\{\{Ag[(1R,2R)\text{-3-bcpb}]\}\cdot X\cdot 3H_2O\}_n$ [X = $NO_3$ (**2a**), $ClO_4$ (**2b**)], have been synthesized by changing the reaction temperature with the structures of **1a** and **1b** as 1D chiral linear chains, as well as **2a** and **2b** as 1D $2_1$ left-handed helical chains with dual chiral components, including the congenital chiral carbon centres and the acquired chirality of the single-handed helices. Meanwhile, **1a** and **1b** can be transformed to **2a** and **2b**, respectively. DFT studies indicated that the configuration of the ligand in **1a** and **1b** is the kinetically favored configuration, while the other configuration in **2a** and **2b** is thermodynamically favored one, which is consistent with the experimental phenomena.

**Materials and Methods.** All solvents and reagents were obtained commercially and used without further purification. (1*R*,2*R*)-3-bpcd was prepared in the similar manner as reported previously.[9b] The synthetic procedure of (1*R*,2*R*)-3-bcpb has been put into the electronic supplementary information.

Infrared (IR) spectroscopic studies have been carried out in the mid-IR region as KBr pellets (Nicolet FT-IR 200). C, H and N microanalyses were made with a Perkin-Elmer 1400C analyzer. Circular dichroism (CD) and emission spectra were collected on a JASCO J-810 and a HORIBA Jobin Yvon Fluoromax-4 spectrophotometer, respectively, at room temperature under air. Powder X-ray diffraction (XRD) intensities were measured on a Rigaku D/max-IIIA diffratometer (CuKα, 1.54056 Å) with a scan rate of $5^o$/min in the range of 3-$60^o$. Thermogravimetric analysis (TGA) was recorded on a 209 F3 Tarsus thermogravimetric analyzer. Kurtz powder method was used to test the second-harmonic generation (SHG) efficiency of the new compounds.

**Synthesis of $\{\{Ag[(1R,2R)\text{-3-bcpb}]\}\cdot NO_3\cdot H_2O\cdot CH_3OH\}_n$ (1a).** **1a** was prepared by adding a methanol solution (10 mL) of (1*R*,2*R*)-3-bcpb (50 mg, 0.1 mmol) to an aqueous solution (10 mL) of

$AgNO_3$ (17 mg, 0.1 mmol). The resulting colorless solution was stirred for half an hour at 25 °C, then filtered. The filtrate was left to evaporate in air under dark at room temperature. After 1 week, colorless block crystals of **1a** were obtained. Yield: 59% based on Ag(I) (43 mg). Anal. Calcd. (%) for $C_{33}H_{38}AgN_5O_7$: C 54.70, H 5.29, N 9.67; found: C 54.66, H 5.33, N 9.72. IR (KBr, $cm^{-1}$): 3447(b, vs), 2940(m), 2860(w), 1630(s), 1430(m), 1410(m), 1380(s), 1310(s), 1260(w), 1110(w), 1080(w), 1030(w), 985(w), 931(w), 793(m), 731(m), 706(s), 663(w), 623(m), 584(w), 528(w), 480(w).

**Synthesis of {{Ag[(1*R*,2*R*)-3-bcpb]}·$ClO_4$·$H_2O$·$CH_3OH$}$_n$ (1b).** The reaction was carried out in an analogous way to that for **1a**, except using $AgClO_4$ (21 mg, 0.1 mmol) instead of $AgNO_3$. The filtrate was left to evaporate in air under dark at room temperature. After 1 week, colorless block crystals of **1b** were obtained in 51% yield based on Ag(I) (39 mg). Anal. Calcd. (%) for $C_{33}H_{38}AgClN_4O_8$: C 52.01, H 5.03, N 7.35; found: C 52.06, H 4.98, N 7.31. FT-IR (KBr, $cm^{-1}$): 3467(b, vs), 2940(m), 2860(w), 1620(s), 1490(w), 1460(m),1430(m), 1410(m), 1380(s), 1320(s), 1260(w), 1170(m), 1160(w), 1110(w), 1080(w), 1050(w), 1030(w), 1010(w), 931(w), 903(w), 825(w), 796(m), 733(m), 704(s), 663(w), 638(m), 594(w), 530(w), 486(w).

**Synthesis of {{Ag[(1*R*,2*R*)-3-bcpb]}·$NO_3$·$3H_2O$}$_n$ (2a).** Method 1: A mixture of $AgNO_3$ (17 mg, 0.1 mmol), (1*R*,2*R*)-3-bcpb (50 mg, 0.1 mmol), $H_2O$ (2 mL) and methanol (8 mL) was heated in a 15-mL Teflon-lined vessel at 90 ºC for 48 hours, followed by slow cooling (5 ºC $h^{-1}$) to room temperature. After filtration, the filtrate was left to evaporate in air under dark at room temperature. Colorless block crystals of **2a** were obtained in 61% yield based on Ag(I) after 2 weeks (42 mg). Anal. Calcd. (%) for $C_{32}H_{38}AgN_5O_8$: C 52.76, H 5.26, N 9.61; found: C 52.74, H 5.23, N 9.66. FT-IR (KBr, $cm^{-1}$): 3456(b, s), 2940(m), 2860(w), 1620(s), 1490(w), 1460(m), 1430(w), 1380(w), 1320(w), 1260(m), 1170(m), 1160(w), 1110(w), 1080(s), 1050(w), 1030(w), 1010(w), 931(w), 866(w), 855(w), 795(m), 733(m), 704(s), 663(w), 638(m), 530(w), 486(w).

Method 2: A mixture of **1a** (100 mg, 0.14 mmol) and methanol (8 mL) was heated in a 15-mL Teflon-lined vessel at 90 ºC for 48 hours, followed by slow cooling (5 ºC $h^{-1}$) to room temperature. After

filtration, the filtrate was left to evaporate in air under dark at room temperature. Colorless block crystals of **2a** were obtained in 69% yield based on Ag(I) after 2 weeks (69 mg).

**Synthesis of {{Ag[(1*R*,2*R*)-3-bcpb]}·$ClO_4$·$3H_2O$}$_n$ (2b).** Method 1: The reaction was carried out in an analogous way to method 1 for **2a**, except using $AgClO_4$ (21 mg, 0.1 mmol) instead of $AgNO_3$. The filtrate was left to evaporate in air under dark at room temperature. After 1 week, colorless block crystals of **2b** were obtained in 51% yield based on Ag(I) (39 mg). Anal. Calcd. (%) for $C_{32}H_{38}AgClN_4O_9$: C 50.18, H 5.00, N 7.31; found: C 50.23, H 4.96, N 7.30. FT-IR (KBr, $cm^{-1}$): 3480(b, vs), 2940(m), 2870(w), 1620(s), 1490(w), 1460(w), 1430(m), 1410(m), 1380(w), 1320(m), 1260(m), 1170(w), 1080(s), 1030(w), 1000(w), 933(w), 860(w), 791(w), 733(m), 706(m), 623(m), 528(w), 428(w).

Method 2: The reaction was carried out in an analogous way to method 2 for **2a**, except using **1b** (100 mg, 0.13 mmol) instead of **1a**. The filtrate was left to evaporate in air under dark at room temperature. After 1 week, colorless block crystals of **2b** were obtained in 75% yield based on Ag(I) (75 mg).

**X-ray Crystallography.** Diffraction intensities for the compounds were collected on a Bruker Apex CCD area-detector diffractometer (MoKα, λ = 0.71073 Å). Absorption corrections were applied by using multiscan propram SADABS.[18] The structures were solved with direct methods and refined with full-matrix least-squares technique using the SHELXTL program package.[19] Anisotropic thermal parameters were applied to the non-hydrogen atoms, except for disordered C, Cl, N and O atoms. The hydrogen atoms on C and N atoms were generated geometrically. The assignment of the absolute structures for **1a**, **1b**, **2a** and **2b** was confirmed by the refinement of Flack enantiopole parameter to values of -0.03(5), 0.00(4), 0.05(5) and -0.04(7), respectively.[20] The nitrate and methanol in **1a**, the three free water molecules in **2a**, the perchlorate and methanol in **1b**, as well as the perchlorate and the free water molecules in **2b** were badly disordered. N-O and Cl-O bond lengths, as well as O-N-O and O-Cl-O bond angles of the disordered nitrate and perchlorate anions were restrained to chemically reasonable

using the DFIX commands on *SHELXL-97*. The disordered nitrate and methanol in **1a**, disordered nitrate and three free water molecules in **2a**, disordered methanol in **1b**, as well as disordered perchlorate in **2b** were restrained as the same thermal displacement parameter, respectively, using the EADP command on *SHELXL-97*. Isotropic thermal parameters were applied to the non-hydrogen atoms of disordered nitrate and methanol in **1a**, the O and C atoms of the disordered methanol in **1b**, as well as the O atoms of the three disordered water molecules in **2a** and **2b**. Residual electron densities greater than 1 e/$A^3$ for **1a** (1.967) and **1b** (2.062) may be attributed to the disordered methanol molecules. Crystal data as well as details of data collection and refinements for the complexes are summarized in Table 1. Selected bond distances and bond angles are listed in Table S1, and hydrogen bonding parameters are given in Table S2.

**Computational details.** The GAUSSIAN 09 program[21] package was employed to carry out DFT[22] calculations at the Becke's three-parameter functional and Lee-Yang-Parr functional (B3LYP) level[23] of calculation, and the 6-31G(d) basis set[24] was used for ground state geometry optimization.

## Results and Discussion

**Synthesis**. The synthesis is summarized in Scheme 3. The reaction conditions employed for the preparations of all the complexes were relatively simple and similar. The compounds were prepared from the mixture of (1*R*,2*R*)-3-bcpb, the corresponding Ag(I) salt, $CH_3OH$ and $H_2O$. The difference of synthetic procedures of **1a** and **1b**, as well as **2a** and **2b**, respectively, is the counteranion, which has no effect on the frameworks of the resultant CCPs; while the difference of synthetic procedures between **1a**(**1b**) and **2a**(**2b**) is the reaction temperature, which highly affects the final structures of CCPs. When the reactions were undertaken at 25 and 90 °C, respectively, two pairs of CCPs based on different counteranions, are obtained, in which **1a** and **1b** are isomorphous with 1D linear chain, while **2a** and **2b** display a 1D left-handed $2_1$ helical chain. This may be attributed to the different configuration of the ligand in **1a**(**1b**) and **2a**(**2b**). Interestingly, **1a** and **1b** can be directly transformed to **2a** and **2b**, respectively, by heating at 90 °C in methanol, while the reverse operations failed to obtain **1a** and **1b**

from **2a** and **2b**, respectively, by heating at 25 °C, which shows that **2a** and **2b** are thermodynamically favored conformers.

Infrared spectra of the compounds display that the strong peaks of 2940 and 2860 (or 2870) $cm^{-1}$ for the four complexes can be attributed to the C-H stretching vibration.[19] Meanwhile, strong broad absorption band at 1380 $cm^{-1}$ for **1a** and **1b**, is consistent with the vibration of the nitrate groups.[19a] The strong absorption band at 1080 $cm^{-1}$ for **2a** and **2b** can be ascribed to the vibration of perchlorates.[19b] The strong absorption band in the 1630 for **1a** and 1620 $cm^{-1}$ for **1b**, **2a** and **2b** is in accordance with the vibrations of C=O groups for the complexes.

**Crystal structures of 1a and 1b.**

Single-crystal XRD study revealed that $\{\{Ag[(1R,2R)\text{-3-bcpb}]\}\cdot X\cdot H_2O\cdot CH_3OH\}_n$ [X = $NO_3$ (**1a**), $ClO_4$ (**1b**)] crystallizes in a triclinic system with space group *P*1. Since the crystals of **1a** and **1b** are isomorphous, only the structure of **1a** is depicted in detail. The asymmetric unit of **1a** contains one (1*R*,2*R*)-3-bcpb ligand, one Ag(I) ion, one nitrate, one weakly coordinated water molecule and one free methanol molecule. Each Ag(I) ion displays an approximately linear geometry, being surrounded by two pyridyl nitrogen atoms of two adjacent ligands with Ag-N distances of 2.233(11) and 2.258(12) Å, and the N-Ag-N angle of 152.4(4) °. Meanwhile, each Ag(I) ion has weak contacts with one nearby water molecule and one nitrate with Ag···O distance of 2.613(8) and 2.632(13) Å, respectively. Each (1*R*,2*R*)-3-bcpb ligand has a bidentate mode in **1a** and bridges two Ag(I) ions to form a 1D chain running along the crystallographic [101] direction with the shortest intrachain Ag···Ag distance of 14.511(2) Å. From the topological view, each Ag(I) can be considered as a two-connecting node, which is connected by the bridging organic ligands as two-connecting linkers. Consequently, the 1D chain can be regarded as a linear chain (Fig. 1b). It is worth noting that each (1*R*,2*R*)-3-bcpb ligand in **1a** adopts a *trans* coordination mode to link two Ag(I), and two pairs of pyridyl and phenyl rings on the same sides of the ligand are inclined to mutual perpendicularity with the angles of 84.04(2) and 63.51(3)º, respectively,

while the two pyridyl rings are inclined to mutual parallelism with the angle between them of 20.24(1)º (Fig 2a).

The 1D chains are further constructed into a two-dimensional (2D) supramolecular network along the *ac* plane *via* interchain O-H···O hydrogen bonds between the weakly coordinated water molecules and adjacent oxygen atoms of C=O with the O···O distance of 2.832(14) Å (Fig. S1).

**Crystal structures of 2a and 2b.**

The crystals of **2a** and **2b** are isomorphous, only the structure of **2a** is depicted in detail. Complex **2a** crystallizes in an orthorhombic system of space group $P2_12_12_1$, consisting of one Ag(I) ion, one (1*R*,2*R*)-3-bcpb ligand, one weakly coordinated perchlorate and three free water molecules in an asymmetric unit. Similar to that in **1a**, each Ag(I) ion in **2a** is linearly coordinated by two pyridyl nitrogen atoms from two adjacent ligands with Ag-N distances of 2.165(5) and 2.147(5) Å, as well as the angle of N-Ag-N of 167.55(19) º. Moreover, each Ag(I) ion has a weak contact with one nearby nitrate with Ag···O distance of 2.707(2) Å. Each (1*R*,2*R*)-3-bcpb ligand acts in a bidentate mode in **2a**, bridging two adjacent Ag(I) ions in the *cis* fashion (Fig. 2b) into a left-handed $2_1$ helical chain running along the crystallographic *c* axis (Fig. 3). It's noteworthy that the helical chain in **2a** is left-handed, being different from that in the 1D right-handed $\{\{Cu[(1R,2R,N^1S,N^2S)\text{-3-bpcd}]\}.NO_3.H_2O\}_n$,[9a] which is also based on (1*R*,2*R*)-1,2-diaminocyclohexane derivatives. In the $2_1$ helical chain, the shortest intrachain Ag···Ag distance is 13.836(1) Å, being a little shorter than that in **1a** (14.511(2) Å), and the screw pitch is 23.209(1) Å. Besides the different coordination mode of the (1*R*,2*R*)-3-bcpb ligand in **1a** and **2a**, the relationship of two pairs of pyridyl and phenyl rings on the same sides of the ligand in **2a** are also different from those in **1a**: in one side, the pyridyl ring is inclined to be parallel to the phenyl ring with the angle between them is 24.54(1)º; while in the other side, the pyridyl and phenyl rings are inclined to mutual perpendicularity with the angle between them of 45.36(2)º (Fig. 2b). The two pyridyl rings of the ligand in **2a** are inclined to be mutual perpendicular with the angle of 85.12(2)º, being also different from that in **1a** (Fig 2).

On the other hand, there are three free water molecules in each asymmetric unit, which are connected with each other *via* hydrogen bonds [O1w···O2w 2.73(3), O2w···O3w 2.75(4) and O3w···O1w 2.86(4) Å] into an infinite left-handed $2_1$ helical chain running along the crystallographic *b* axis, which is also vertical to the $2_1$ helix of the coordination polymer (Fig. 4a). Additionally, the $2_1$ water helical chains link the left-handed $2_1$ helices of the coordination polymer into a 3D hydrogen bonding network *via* O-H···O hydrogen bonds between the free water molecules and the oxygen atoms of C=O in the ligands with the O···O distance of 2.77(3) Å (Fig. 4b).

**Geometry optimization and DFT studies**

In order to make clear the relationship between the configurations of the ligand and reaction temperature in theory, here the two kinds of molecular geometries of the (1*R*,2*R*)-3-bcpb ligand in the four complexes were optimized by Density functional calculations, by employing the GAUSSIAN 09 suite of programs at the B3LYP level (Fig. 5). The 6-31G(d) basis set was used for ground state geometry optimization. From the optimized geometry and stabilization energy values, it is clear that the configuration of the ligand in linear complexes **1a** and **1b**, with a single point energy (SPE) = -1607.72 a.u., is the kinetically favored configuration and the other configuration of the ligand in helical complexes **2a** and **2b**, with a SPE = -1607.54 a.u., is the thermodynamically favored one. The calculation results are in agreement with experimental phenomena, in which the linear chains appeared in the lower temperature (25 °C), while the helical chains were obtained in the higher temperature (90 °C), as well as **1a** and **1b** can be directly transformed to **2a** and **2b**, respectively, by heating, while the reverse operations failed.

**Thermogravimetric analysis and Powder X-ray diffraction**

Because of the easy explosion of perchlorates at high temperature, only the TGA of complexes **1a** and **2a** were performed under $N_2$ atmosphere with a heating rate of 10 ºC $min^{-1}$. The thermal decompositions of the two complexes are consistent with the crystallographic observations (Fig. 6). For

**1a**, the initial weight loss of 3.8% from room temperature to 96 ºC indicates the removal of the free methanol and water molecules (calc. 6.9%). Then, the structure without the solvent molecules is maintained until 163 ºC. The weight loss of 74.0 % in the range of 163 to 340 ºC corresponds to the release of the organic ligands (calc. 69.6%) and the collapse of the whole structure. For **2a**, there are also two steps of obvious weight losses. The first one from 26 to 186 ºC corresponds to the loss of the free water molecules. The observed weight loss of 5.9% is in agreement with the calculated value of 7.4%. The second weight loss of 77.9% (calc. 69.3%) from 186 to 320 ºC corresponds to the removal of ligands and the decomposition of the whole framework.

Phase purity of bulk of the crystalline samples of **1a**, **1b**, **2a** and **2b** was confirmed by a good match between the experimental and simulated powder X-ray diffraction (PXRD) patterns, as shown in Fig. S2-S5.

**Luminescent Properties**

Ag(I) compounds usually exhibit interesting luminescent properties.[9,25] Thus, the luminescent spectra of the ligand, as well as the complexes **1a**, **1b**, **2a** and **2b** in the solid state, were investigated at room temperature, as shown in Fig. 7. The ligand exhibits an intense UV radiation with $\lambda_{max}$ at 275 nm upon excitation at 485 nm, which may be attributed to $\pi$–$\pi^*$ transition. Upon excitation at 270 nm, **1a** and **1b** exhibit a similar cyan luminescence emission at 486 and 482 nm, while **2a** and **2b** show a cyan photoluminescence emission at 484 and 492 nm upon excitation at 277 nm, respectively. Compared with the emissions of the free ligand, the slight blue-shift (3-7 nm) of the four complexes may be assigned to the intraligand transitions;[26] the enhancement in **1a** and **1b** is probably attributable to the strong interaction between the Ag(I) and the ligand, or increasing rigidity due to the coordination, effectively reducing the loss of energy by nonradiative decay.[25] Interestingly, the weakened luminescent intensities of **2a** and **2b**, which are lower than the ligand, and are only *ca.* 1/5 and 1/10 of **1a** and **1b**, respectively, which may be attributed to the different configurations of the ligand in the 1D linear and helical chains.

**Circular dichroism spectra and second-harmonic generation**

Circular dichroism (CD) spectroscopy is widely used in the construction of CCPs to check the chirality of bulk crystals. The chiral nature of (1*R*,2*R*)-3-bcpb and the four CCPs was confirmed by solid state CD spectroscopy using powdered bulk crystals in a KBr matrix between 200 and 500 nm at room temperature (Fig. 8). The ligand shows dichroic signals in its CD spectra with a positive Cotton effect at frequency of 253 nm, while the two pairs of isomorphous complexes **1a** and **1b**, as well as **2a** and **2b**, respectively, were found to display similar dichroic signals. **1a** and **1b** show similar signals with two positive Cotton effects at frequencies of 252 and 299 nm, 245 and 291 nm, and a negative Cotton effect at the frequency of 268 nm and 271 nm, respectively; while **2a** and **2b** show similar signals with two positive Cotton effects at the 221 and 248 nm, 212 and 250 nm frequencies, and a negative Cotton effect at the 226 and 218 nm frequencies, respectively. The measurements were repeated on the crystals from different batches, which showed similar CD signals.

Second harmonic generation (SHG) active CPs, combining the advantages of the metal ions and organic ligands, have attracted considerable interest because of their potential applications in light modulators, electric-optical devices and information storage.[27] **1a**, **1b**, **2a** and **2b** are all CCPs with noncentrosymmetric crystal structures. Therefore, their second-order NLO properties are worth studying. SHG measurements on powder samples of the four compounds mentioned above were carried out by the Kurtz-Perrymethod[28] at room temperature, in order to confirm their chirality and evaluate their potential application as second-order NLO materials. The results show that **1a**, **1b**, **2a** and **2b** are SHG-active, with approximately 0.2, 0.2, 0.3 and 0.3 times as big as that of KDP, respectively, which evaluates their potential as second-order nonlinear optical materials. The modest powder SHG response of the four complexes may be attributed to a comparable short donor-acceptor system, which is essential for second-order optical nonlinearity.[9]

**Conclusion**

In this work, we have synthesized two pairs of chiral coordination polymers with the same materials at 25 and 90 °C, respectively. **1a** and **1b**, as well as **2a** and **2b** are supramolecular isomers, respectively, exhibiting a 1D chiral linear chain and a left-handed $2_1$ helical chains. **1a** and **1b** can be transformed to **2a** and **2b**, respectively, by heating at 90 °C in methanol; while the reverse operations failed. The different structures of **1a** (**2a**) and **1b** (**2b**) may be attributed to the different configurations of the ligand, which are highly affected by the reaction temperature. DFT calculations verified the experimental observations in theory. CD spectra and SHG efficiency measurement confirmed that the bulk samples were chiral. All the products also display strong solid-state luminescent emission. The present research demonstrates that temperature is a crucial factor for the construction of CCPs.

**Acknowledgment.** The authors are grateful to the financial support from National Natural Science Foundation of China (No. 21001024 and 21471031), the Natural Science Foundation of Jiangsu Province (BK2011587 and BK20131289), the Funding from Southeast University (No. 4007041121 and No. 9207040016) and Key lab of Novel Thin film Solar Cells (KF201112).

**Electronic supplementary information (ESI) available:** PXRD plots of the four CCPs. The synthesis of (1*R*,2*R*)-3-bcpb. Selected bond distances and bond angles, as well as hydrogen bonding parameters of the four complexes. X-ray crystallographic file in CIF format for **1a**, **1b**, **2a** and **2b**. CCDC reference numbers 1013603-1013606 for **1a**, **2a**, **1b** and **2b**, respectively. For ESI and crystallographic data in CIF or other electronic format see DOI: xx.xxxx/xxxxxxxxxx.

**Notes and references**

1 (a) O. M. Yaghi, M. O'Keeffe, N. W. Ockwig, H. K. Chae, M. Eddaoudi and J. Kim, *Nature*, 2003, **423**, 705; (b) J. S. Seo, D. Whang, H. Lee, S. I. Jun, J. Oh, Y. J. Jeon and K. Kim, *Nature*, 2000, **404**, 982; (c) D. Bradshaw, J. B. Claridge, E. J. Cussen, T. J. Prior and M. J. Rosseinsky,

*Acc. Chem. Res.*, 2005, **38**, 273; (d) G. Férey, *Chem. Soc. Rev.*, 2008, **37**, 191; (e) J. Crassous, *Chem. Soc. Rev.*, 2009, **38**, 830; (f) J. Jacques, A. Collet and S. H. Wilen, *Enantiomers, Racemates and resolutions*, Wiley-VCH, New York, 1981; (g) H. Amouri, M. Gruselle, D. Woollins, D. A. Atwood, R. H. Crabtree and G. Mayer, *Chirality in Transition Metal Chemistry: Molecules, Supramolecular Assemblies and Materials*, Wiley-VCH, New York, 2008; (h) X. L. Yang and C. D. Wu, *CrystEngComm*, 2014, **16**, 4907.

2 (a) S. Kitagawa, R. Kitaura and S. Noro, *Angew. Chem. Int. Ed.*, 2004, **43**, 2334; (b) S. J. Lee, A. G. Hu and W. B. Lin, *J. Am. Chem. Soc.*, 2002, **124**, 12948; (c) J. Heo, Y. M. Jeon and C. A. Mirkin, *J. Am. Chem. Soc.*, 2007, **129**, 7712; (d) J. Zhang, S. M. Chen, T. Wu, P. Y. Feng and X. H. Bu, *J. Am. Chem. Soc.*, 2008, **130**, 12882; (e) C. Train, T. Nuida, R. Gheorghe, M. Gruselle and S. I. Ohkoshi, *J. Am. Chem. Soc.*, 2009, **131**, 16838; (f) K. K. Bisht and E. Suresh, *J. Am. Chem. Soc.*, 2013, **35**, 15690; (g) Y. Q. Hu, M. H. Zeng, K. Zhang, S. Hu, F. F. Zhou, M. Kurmoo, *J. Am. Chem. Soc.*, 2013, **135**, 7901.

3 (a) M. H. Zeng, B. Wang, X. Y. Wang, W. X. Zhang, X. M. Chen and S. Gao, *Inorg. Chem.*, 2006, **45**, 7069; (b) F. Li, T. H. Li, X. J. Li, X. Li, Y. L. Wang and R. Cao, *Cryst. Growth Des.*, 2006, **6**, 1458; (c) Y. Ma, Z. B. Han, Y. K. He and L. G. Yang, *Chem. Commun.*, 2007, 4107; (d) J. J. Wu, M. L. Cao and B. H. Ye, *Chem. Commun.*, 2010, **46**, 3687; (e) X. L. Tong, T. L. Hu, J. P. Zhao, Y. K. Wang, H. Zhang and X. H. Bu, *Chem. Commun.*, 2010, **46**, 8543; (f) Z. B. Hang, B. Y. Li, J. W. Ji, Y. E. Du, H. Y. An and M. H. Zeng, *Dalton Trans.*, 2011, **40**, 9154; (g) P. Zhou, J. F. Yao, C. F. Sheng and H. Li, *CrystEngComm*, 2013, **15**, 8430; (h) M. H. Zeng, Y. X. Tan, Y. P. He, Z. Yin, Q. Chen and M. Kurmoo, *Inorg. Chem.*, 2013, **52**, 2353; (i) Y. H. Wen, T. L. Sheng, Z. H. Sun, Z. Z. Xue, Y. L. Wang, Y. Wang, S. M. Hu, X. Ma and X. T. Wu, *Chem. Commun.*, 2014, **50**, 8320.

4 (a) L. Hou, J. P. Zhang, X. M. Chen and S. W. Ng, *Chem. Commun.*, 2008, 4019; (b) Z. B. Han, Y. K. He, M. L. Tong, Y. J. Song, X. M. Song and L. G. Yang, *CrystEngComm,* 2008, **10**, 1070; (c) Y. H. Xu, Y. Q. Lan, S. X. Wu, K. Z. Shao, Z. M. Su and D. Liao, *CrystEngComm*, 2009, **11**, 1711; (d) Y. L. Zhou, F. Y. Meng, J. Zhang, M. H. Zeng and H. Liang, *Cryst. Growth Des.*, 2009, **9**, 1402; (e) G. Dura, M. C. Carrion, F. A. Jalon, A. M. Rodriguez and B. R. Manzano, *Cryst. Growth Des.*, 2013, **13**, 3275; (f) K. H. Park, T. H. Noh, Y. B. Shim and O. S. Jung, *Chem. Commun.*, 2013, **49**, 4000; (g) Y. Y. Yin, Y. L. Zhao, J. G. Ma, X. C. Cao and P. Cheng, *Inorg. Chem.*, 2013, **52**, 3738; (h) J. Ru, F. Gao, T. Wu, M. X. Yao, Y. Z. Li and J. L. Zuo, *Dalton Trans.*, 2014, **43**, 933.

5 (a) S. P. Anthony and T. P. Radhakrishnan, *Cryst. Growth Des.*, 2004, **6**, 1223; (b) W. Lewis and P. J. Steel, *Supramol. Chem.*, 2005, **17**, 579; (c) X. Ouyang, Z. X. Chen, X. F. Liu, Y. T. Yang, M. L. Deng, L. H. Weng, Y. M. Zhou and Y. Jia, *Inorg. Chem. Commun.*, 2008, **11**, 948; (d) S. M. Chen, J. Zhang and X. H. Bu, *Inorg. Chem.*, 2009, **48**, 6356; (e) M. Wang, M. H. Xie, C. D. Wu and Y. G. Wang, *Chem. Commun.*, **2009**, **45**, 2396; (f) P. Gou, *Dalton Trans.*, 2011, **40**, 1716; (g) C. M. Nagaraja, R. Haldar, T. K. Maji and C. N. R. Rao, *Cryst. Growth Des.*, 2012, **12**, 975; (h) J. Zhang, S. Gao, X. X. Zhang, Z. M. Wang and C. M. Chi, *Dalton Trans.*, 2012, **41**, 2626; (i) K. Tanaka, A. Asakura, T. Muraoka, P. Kalickib and Z. Urbanczyk-Lipkowskab, *New J. Chem.*, 2013, **37**, 2851; (j) M. J. Kobyłka, K. Š lepokura, M. A. Rodicio, M. Paluch and J. Lisowski, *Inorg. Chem.*, 2013, **52**, 12893; (k) G. Ilyashenko, G. De Faveri, T. Follier, R. Al-Safadi, M. Motevalli and M. Watkinson, *Org. Biomol. Chem*., 2014, **12**, 1124.

6 (a) L. X. Dai, *Angew. Chem. Int. Ed.*, 2004, **43**, 5726; (b) Z. R. Qu, H. Zhao, Y. P. Wang, X. S. Wang, Q. Ye, Y. H. Li, R. G. Xiong, B. F. Abrahams, Z. G. Liu, Z. L. Xue and X. Z. You, *Chem. Eur. J.*, 2004, **10**, 53; (c) M. Kato, A. K. Sah, T. Tanase and M. Mikuriya, *Eur. J. Inorg. Chem.*, 2006, 2504; (d) H. Y. Liu, B. Zhao, W. Shi, Z. J. Zhang, P. Cheng, D. Z. Liao and S. P. Yan,

*Eur. J. Inorg. Chem.*, 2009, 2599; (e) G. Q. Zhang, E. Yashima and W. D. Woggona, *Adv. Synth. Catal.*, 2009, **351**, 1255; (f) S. M. Shin, D. Moon, K. S. Jeong, J. Kim, P. K. Thallapally and N. Jeong, *Chem. Commun.*, 2011, **47**, 9402; (g) A. C. Kathalikkattil, P. S. Subramanian and E. Suresh, *Inorg. Chim. Acta*, 2011, **365**, 363; (h) A. Gerus, K. Š lepokura and J. Lisowski, *Inorg. Chem.*, 2013, **52**, 12450; (i) G. Q. Zhang, *Inorg. Chem. Commun.*, 2014, **40**, 1.

7 (a) M. Seitz, A. Kaiser, S. Stempfhuber, M. Zabel and O. Reiser, *J. Am. Chem. Soc.*, 2004, **126**, 11426; (b) H. R. Wen, C. F. Wang, Y. Song, J. L. Zuo and X. Z. You, *Inorg. Chem.*, 2005, **44**, 9039; (c) A. R. Geisheimer, M. J. Katz, R. J. Batchelor and D. B. Leznoff, *CrystEngComm*, 2007, **9**, 1078; (d) L. Wang, W. You, W. Huang, C. Wang and X. Z. You, *Inorg. Chem.*, 2009, **48**, 4295; (e) W. Y. Wang, X. L. Niu, Y. C. Gao, Y. Y. Zhu, G. Li, H. J. Lu and M. S. Tang, *Cryst. Growth Des.*, 2010, **10**, 4050; (f) R. Saha, S. Biswas and G. Mostafa, *CrystEngComm*, 2011, **13**, 1018; (g) S. C. Xiang, Z. J. Zhang, C. G. Zhao, K. L. Hong, X. B. Zhao, D. R. Ding, M. H. Xie, C. D. Wu, M. C. Das, R. Gill, K. M. Thomas and B. L. Chen, *Nat. Commun.*, 2011, **2**, 204; (h) W. M. Xuan, C. C. Ye, M. N. Zhang, Z. J. Chen and Y. Cui, *Chem. Sci.*, 2013, **4**, 3154; (i) N. Ch. Maity, P. K. Bera, D. Ghosh, S. H. R. Abdi, R. I. Kureshy, N. H. Khan, H. C. Bajajab and E. Suresh, *Catal. Sci. Technol.*, 2014, **4**, 208.

8 (a) R. T. Yin, Z. Cao and L. Cheng, *Acta Cryst.*, 2011, **E67**, m392; (b) C. Z. Gao, X. Y. Zhang and L. Cheng, *Acta Cryst.*, 2012, **E68**, m235.

9 (a) L. Cheng, L. M. Zhang, S. H. Gou, Q. N. Cao, J. Q. Wang and L. Fang, *CrystEngComm*, 2012, **14**, 3888; (b) L. Cheng, L. M. Zhang, S. H. Gou, Q. N. Cao, J. Q. Wang and L. Fang, *CrystEngComm*, 2012, **14**, 4437; (c) L. Cheng, L. M. Zhang, Q. N. Cao, S. H. Gou, X. Y. Zhang and L. Fang, *CrystEngComm*, 2012, **14**, 7502; (d) L. Cheng, Q. N. Cao, X. Y. Zhang, S. H. Gou and L. Fang, *Inorg. Chem. Commun.*, 2012, **24**, 110; (e) L. Cheng, Q. N. Cao, L. M. Zhang, X.

Y. Zhang, S. H. Gou and L. Fang, *Solid State Sci.*, 2013, **16**, 34; (f) X. Y. Zhang, L. Cheng, J. Wang, S. H. Gou and L. Fang, *Inorg. Chem. Commun.*, 2014, **40**, 97.

10 (a) L. Cheng, J. B. Lin, J. Z. Gong, A. P. Sun, B. H. Ye and X. M. Chen, *Cryst. Growth Des.*, 2006, **6**, 2739; (b) S. Hu, H. H. Zou, M. H. Zeng, Q. X. Wang and H. Liang, *Cryst. Growth Des.,* 2008, **8**, 2346; (c) Y. L. Zhou, M. H. Zeng, X. C. Liu, H. Liang and M. Kurmoo, *Chem. Eur. J.,* 2011, **17**, 14084; (d) J. Xiao, B. Y. Liu, G. Wei and X. C. Huang, *Inorg. Chem.,* 2011, **50**, 11032; (e) M. Y. Zhang, W. J. Shan and Z. B. Han, *CrystEngComm,* 2012, **14**, 1568; (f) J. P. Zhang, Y. B. Zhang, J. B. Lin and X. M. Chen, *Chem. Rev.,* 2012, **112**, 1001.

11 (a) J. Yang, N. Lu, G. Zhang, L. Cheng and S. H. Gou, *Polyhedron*, 2008, **27**, 2119; (b) L. Cheng, S. H. Gou and G. Xu, *J. Mol. Struct*., 2010, **979**, 214; (c) H. Shen, L. Cheng, H. Z. Dong, H. B. Zhu, S. H. Gou and X. T. Chen, *Solid State Sci.*, 2010, **12**, 367; (d) L. Cheng, S. H. Gou and L. M. Zhang, *Solid State Sci.*, 2010, **12**, 2163; (e) L. Cheng, S. H. Gou and J. Q. Wang, J. *Mol. Struct.*, 2011, **991**, 149.

12 (a) D. F. Sun, Y. X. Ke, T. M. Mattox, B. A. Ooro and H. C. Zhou, *Chem. Commun.*, 2005, 5447; (b) Y. B. Dong, Y. Y. Jiang, J. Li, J. P. Ma, F. L. Liu, B. Tang, R. Q. Huang and S. R. Batten, *J. Am. Chem. Soc.*, 2007, **129**, 4520; (c) T. Jiang and X. M. Zhang, *Cryst. Growth Des.*, 2008, **8**, 3077; (d) J. J. Wu, W. Xue, M. L. Cao, Z. P. Qiao and B. H. Ye, *CrystEngComm*, 2011, **13**, 5495; (e) L. L. Liu, Z. G. Ren, L. W. Zhu, H. F. Wang, W. Y. Yan and J. P. Lang, *Cryst. Growth Des.*, 2011, **11**, 3479; (f) S. Gao, R. Q. Fan, L. S. Qiang, P. Wang, S. Chen, X. M. Wang and Y. L. Yang, *CrystEngComm*, 2014, **16**, 1113.

13 (a) B. L. Chen, N. W. Ockwig, F. R. Fronczek, D. S. Contreras and O. M. Yaghi, *Inorg. Chem.,* 2005, **44**, 181; (b) X. F. Wang, Y. B. Zhang, W. Xue, X. L. Qi and X. M. Chen, *CrystEngComm*, 2010, **12**, 3834; (c) Z. G. Gu, G. Z. Li, P. Y. Yin, Y. N. Chen, H. M. Peng, M. F. Wang, F. Cheng, F. L. Gu, W. S. Li and Y. P. Cai, *Inorg. Chem. Comm.*, 2011, **14**, 1479; (d) C. Y. Xu, L.

K. Li, Q. Q. Guo, H. W. Hou and Y. T. Fan, *Inorg. Chem. Comm.*, 2011, **14**, 1204; (e) H. C. Fang, Y. Y. Ge, H. Y. Jia, S. S. Li, F. Sun, L. G. Zhang and Y. P. Cai, *CrystEngComm*, 2011, **13**, 67; (f) F. Yu and B. Li, *CrystEngComm*, 2011, **13**, 7025; (g) M. Chen, Y. Lu, J. Fan, G. C. Lv, Y. Zhao, Y. Zhang and W. Y. Sun, *CrystEngComm*, 2012, **14**, 2015; (h) B. Liu, L. Wei, N. N. Li, W. P. Wu, H. Miao, Y. Y. Wang and Q. Z. Shi, *Cryst. Growth Des.*, 2014, **14**, 1110.

14 (a) H. R. Khavasi and B. M. M. Sadegh, *Inorg. Chem.,* 2010, **49**, 5356; (b) S. Wang, Y. Q. Peng, X. L. Wei, Q. F. Zhang, D. Q. Wang, J. M. Dou, D. C. Li and J. F. Bai, *CrystEngComm,* 2011, **13**, 5313; (c) K. L. Zhang, C. T. Hou, J. J. Song, Y. Deng, L. Li, S. W. Ng and G. W. Diao, *CrystEngComm,* 2012, **14**, 590.

15 W. L. Leong and J. J. Vittal, *Chem. Rev.*, 2011, **111**, 688.

16 (a) P. M. Forster, A. R. Burbank, C. Livage, G. Férey and A. K. Cheetham, *Chem. Commun.*, 2004, 368; (b) C. Livage, C. Egger and G. Férey, *Chem. Mater.*, 2001, **13**, 410; (c) D. B. Cordes, L. R. Hanton and M. D. Spicer, *Inorg. Chem.*, 2006, **45**, 7651.

17 (a) X. C. Huang, J. P. Zhang and X. M. Chen, *Cryst. Growth Des.*, 2006, **6**, 1194; (b) X. C. Huang, D. Li and X. M. Chen, *CrystEngComm*, 2006, **8**, 351; (c) M. H. Zeng, M. X. Yao, H. Liang and S. W. Ng, *J. Coord. Chem.*, 2007, **60**, 1983; (d) T. L. Hu, W. P. Du, B. W. Hu, J. R. Li, X. H. Bu and R. Cao, *CrystEngComm*, 2008, **10**, 1037; (e) J. L. Du, T. L. Hu, S. M. Zhang, Y. F. Zhang and X. H. Bu, *CrystEngComm*, 2008, **10**, 1866.

18 G. M. Sheldrick, SADABS 2.05, University of Göttingen, 2002.

19 SHELXTL 6.10, Bruker Analytical Instrumentation, Madison, Wisconsin, USA, 2000.

20 H.D. Flack, *Acta Crystallogr. Sect. A*, 1983, **39**, 876.

21 M. J. Frisch, et al. Gaussian 09, Revision A.02, Gaussian, Inc., Wallingford, CT, 2009.

22 (a) W. Kohn and L. Sham, *J. Phys. Rev. B*, 1965, **140**, 1133; (b) A. D. Becke, *J. Chem. Phys.*, 1992, **97**, 9173.

23 (a) A. D. Becke, *J. Chem. Phys.*, 1993, **98**, 5648; (b) R. Ditchfield, W. J. Hehre and J. A. Pople, *J. Chem. Phys.*, 1971, **54**, 724.

24 V. A. Rassolov, J. A. Pople, M. A. Ratner and T. L. Windus, *J. Chem. Phys.*, 1998, **109**, 1223.

25 (a) L. Cheng, Q. N. Cao, X. Y. Zhang, S. H. Gou and L. Fang, *J. Coord. Chem.*, 2013, **66**, 481; (b) Y. Q. Zhao, M. X. Fang, Z. H. Xu, X. P. Wang, S, N. Wang, L. L. Han, X. Y. Li and D. Sun, *CrystEngComm*, 2014, **16**, 3015; (c) C. F. Yan, Y. X. Lin, F. L. Jiang and M. C. Hong, *Inorg. Chem. Commun.*, 2014, **43**, 19.

26 (a) J. Zhang, Z. J. Li, Y. Kang, J. K. Cheng and Y. G. Yao, *Inorg. Chem.*, 2004, **43**, 8085; (b) D. R. Xiao, Y. G. Li, E. B. Wang, L. L. Fan, H. Y. An, Z. M. Su and L. Xu, *Inorg. Chem.*, 2007, **46**, 4158.

27 (a) C. Wang, T. Zhang and W. Lin, *Chem. Rev.*, 2012, **112**, 1084; (b) W. Zhang and R. G. Xiong, *Chem. Rev.*, 2012, **112**, 1163; (c) Y. H. Wen, T. L. Sheng, S. M. Hu, X. Ma, C. H. Tan, Y. L. Wang, Z. H. Sun, Z. Z. Xue and X. T. Wu, *Chem. Commun.*, 2013, **49**, 10644; (d) X. J. Yang, S. S. Bao, M. Ren, N. Hoshino, T. Akutagawa and L. M. Zheng, *Chem. Commun.*, 2014, **50**, 3979; (e) L. H. Cao, Y. L. Wei, Y. Yang, H. Xu, S. Q. Zang, H. W. Hou and T. C. W. Mak, *Cryst. Growth Des.*, 2014, **14**, 1827; (f) L. Wei, Q. Wei, Z. E. Lin, Q. Meng, H. He, B. F. Yang and G. Y. Yang, *Angew. Chem. Int. Ed.*, 2014, **53**, 7188.

28 S. K. Kurtz and T. T. Perry, *J. Appl. Phys.*, 1968, **39**, 3798.

**Table 1.** Crystal data and structure refinements for **1a**, **1b**, **2a** and **2b**.

| Compound | **1a** | **1b** | **2a** | **2b** |
|---|---|---|---|---|
| Formula | $C_{33}H_{38}AgN_5O_7$ | $C_{33}H_{38}AgClN_4O_8$ | $C_{32}H_{38}AgN_5O_8$ | $C_{32}H_{38}AgClN_4O_9$ |
| *FW* | 724.55 | 761.99 | 728.54 | 765.98 |
| Crystal system | triclinic | triclinic | orthorhombic | orthorhombic |
| Space group | *P*1 | *P*1 | $P2_12_12_1$ | $P2_12_12_1$ |
| *a* / Å | 9.0885(19) | 9.1852(15) | 10.9284(12) | 10.9131(16) |
| *b* / Å | 10.008(2) | 10.2742(17) | 13.1429(14) | 13.0435(19) |
| *c* / Å | 10.316(2) | 10.3527(17) | 23.209(2) | 22.908(4) |
| $\alpha$ / º | 84.680(3) | 84.690(2) | 90 | 90 |
| $\beta$ / º | 83.399(3) | 83.518(2) | 90 | 90 |
| $\gamma$ / º | 66.850(3) | 65.526(2) | 90 | 90 |
| *V* / Å$^3$ | 855.9(3) | 882.4(3) | 3333.5(6) | 3260.8(9) |
| *Z* | 1 | 1 | 4 | 4 |
| $D_c$ / g cm$^{-3}$ | 1.406 | 1.434 | 1.452 | 1.560 |
| *T* / K | 123(2) | 123(2) | 123(2) | 123(2) |
| *F*(000) | 374 | 392 | 1504 | 1576 |
| $\mu$ / mm$^{-1}$ | 0.641 | 0.700 | 0.661 | 0.761 |
| Flack x | -0.03(5) | 0.05(5) | 0.00(4) | -0.04(7) |
| $^aR_1$ (I > 2$\sigma$) | 0.0841 | 0.0748 | 0.0594 | 0.0748 |
| $^bwR_2$ (all data) | 0.1811 | 0.1666 | 0.1686 | 0.1693 |

| | | | | |
|---|---|---|---|---|
| GOF | 1.061 | 1.051 | 1.072 | 1.025 |

[a] $R_1 = \sum||F_o|-|F_c||/\sum|F_o|$, [b] $wR_2 = [\sum w(F_o^2-F_c^2)^2/\sum w(F_o^2)^2]^{1/2}$

*Captions for figures*

**Scheme 1** The structures of (1*R*,2*R*)-$N^1$,$N^2$-bis(pyridinylmethyl)cyclohexane-1,2-diamine derivatives (a), (1*R*,2*R*)-3-bpcd (b) and (1*R*,2*R*)-3-bcpb (c).

**Scheme 2** Three potential isomers based on the relationship between the phenyl and pyridyl rings in the *trans*- configuration of (1*R*,2*R*)-3-bcpb.

**Scheme 3** Summary of the synthesis.

**Fig. 1** The structure of the one-dimensional chiral linear chain of **1a** (a) and its topology (b).

**Fig. 2** The *trans* (a) and *cis* (b) coordination modes of (1*R*,2*R*)-3-bcpb ligand in **1a** and **2a**, respectively.

**Fig. 3** The topology of the left-handed $2_1$ helical chain (a) and its packing diagram (b) in **2a**.

**Fig. 4** The 1D left-handed $2_1$ helical water chain (a) and the 3D hydrogen bonding network (b) in **2a**.

**Fig. 5** The contour plots of the relevant HOMO (a, c) and LUMO (b, d) for optimization models of the two configurations of (1*R*,2*R*)-3-bcpb in **1a** (**1b**) and **2a** (**2b**), respectively.

**Fig. 6** TG plots for **1a** and **2a**.

**Fig. 7** Luminescence spectra of (1*R*,2*R*)-3-bcpb and the four CCPs in the solid state at room temperature.

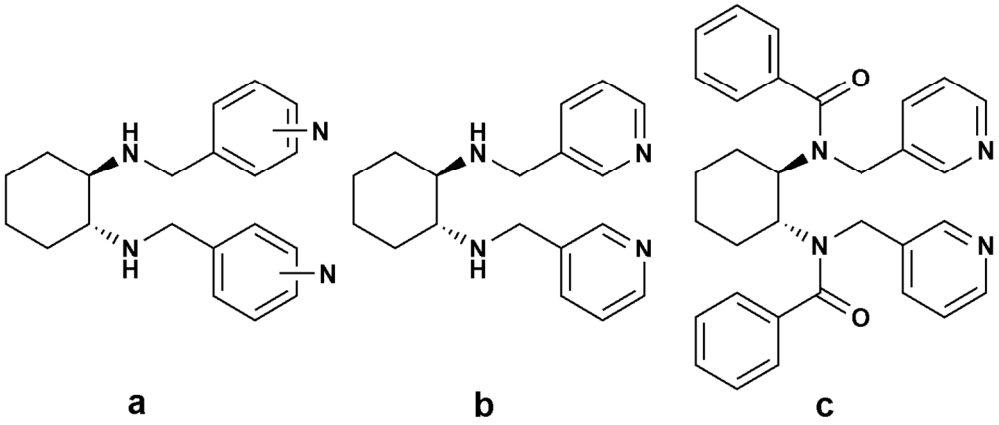


**Scheme 1** The structures of (1*R*,2*R*)-$N^1$,$N^2$-bis(pyridinylmethyl)cyclohexane-1,2-diamine derivatives (a), (1*R*,2*R*)-3-bpcd (b) and (1*R*,2*R*)-3-bcpb (c).
125x53mm (300 x 300 DPI)

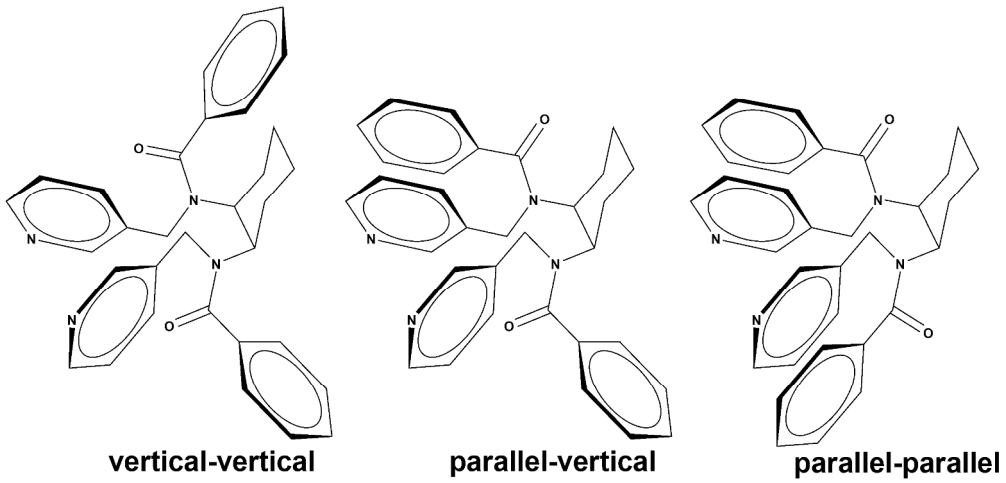


**Scheme 2** Three potential isomers based on the relationship between the phenyl and pyridyl rings in the trans- configuration of (1*R*,2*R*)-3-bcpb.
235x112mm (300 x 300 DPI)

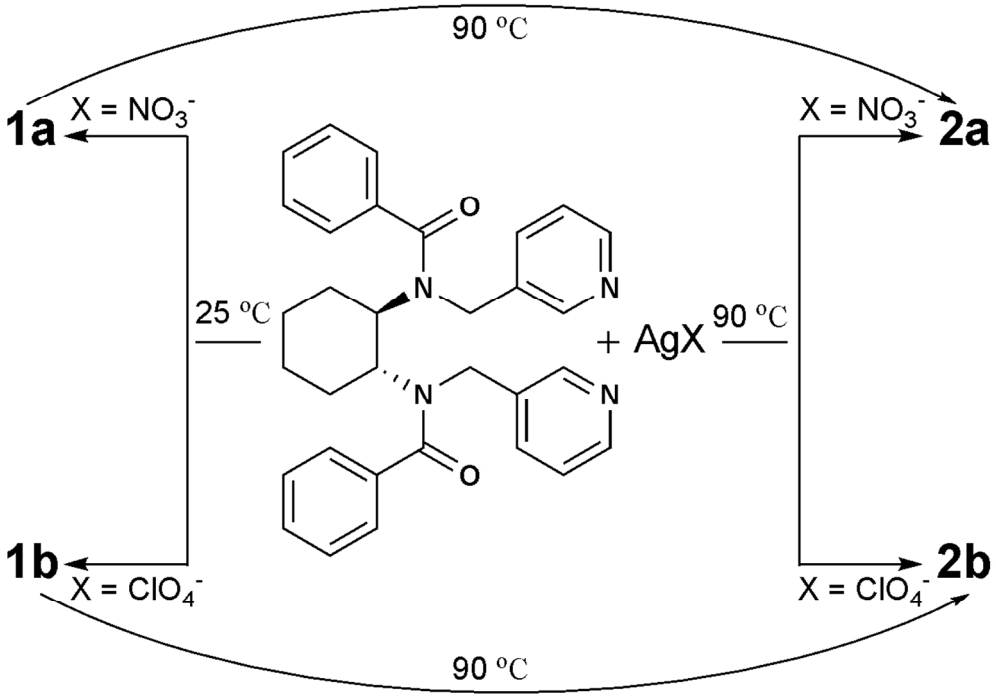


**Scheme 3** Summary of the synthesis.
111x78mm (300 x 300 DPI)

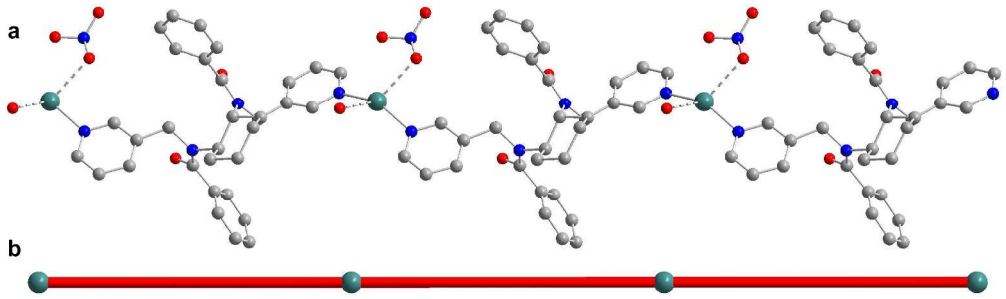


**Fig. 1** The structure of the one-dimensional chiral linear chain of **1a** (a) and its topology (b).
661x193mm (156 x 156 DPI)

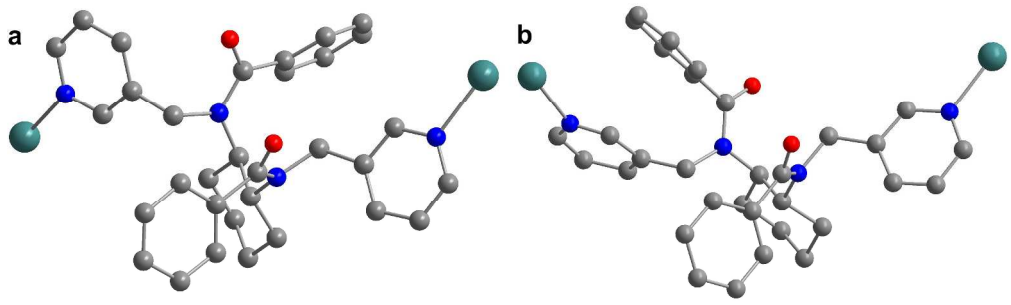


**Fig. 2** The *trans* (a) and *cis* (b) coordination modes of (1*R*,2*R*)-3-bcpb ligand in **1a** and **2a**, respectively.
781x232mm (132 x 132 DPI)

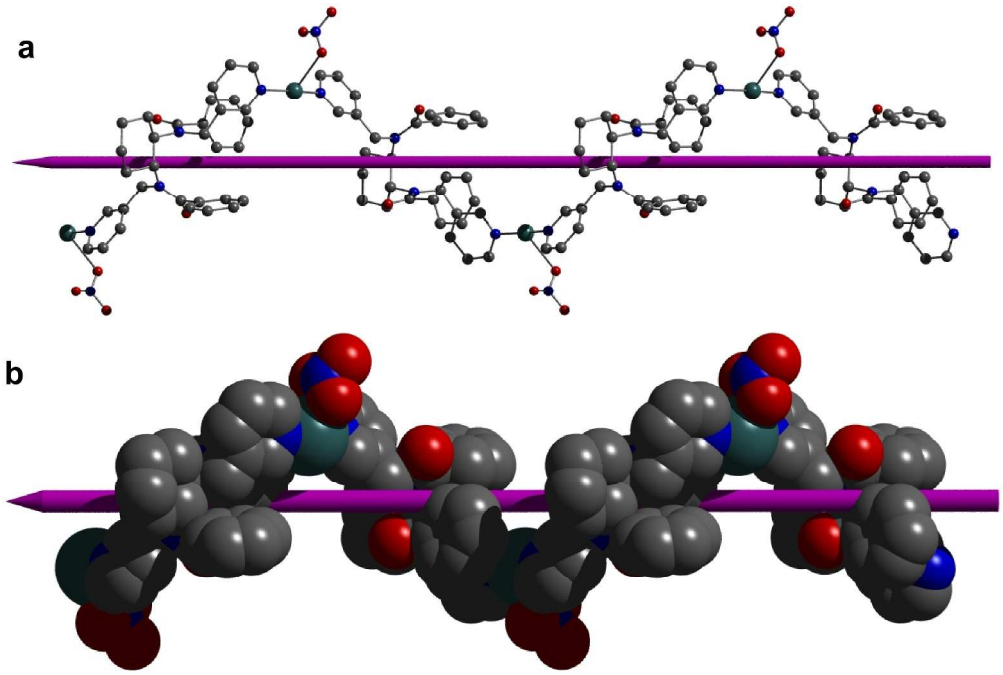


**Fig. 3** The topology of the left-handed $2_1$ helical chain (a) and its packing diagram (b) in **2a**.
701x468mm (145 x 145 DPI)

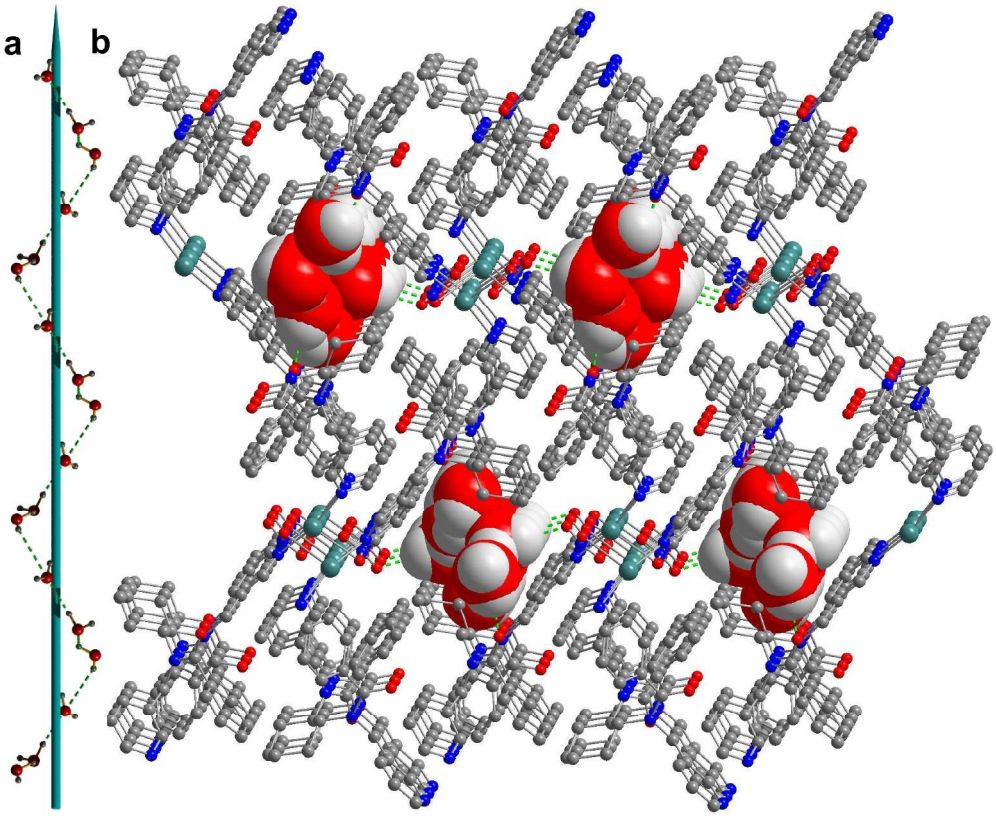


**Fig. 4** The 1D left-handed $2_1$ helical water chain (a) and the 3D hydrogen bonding network (b) in **2a**.
538x439mm (180 x 180 DPI)

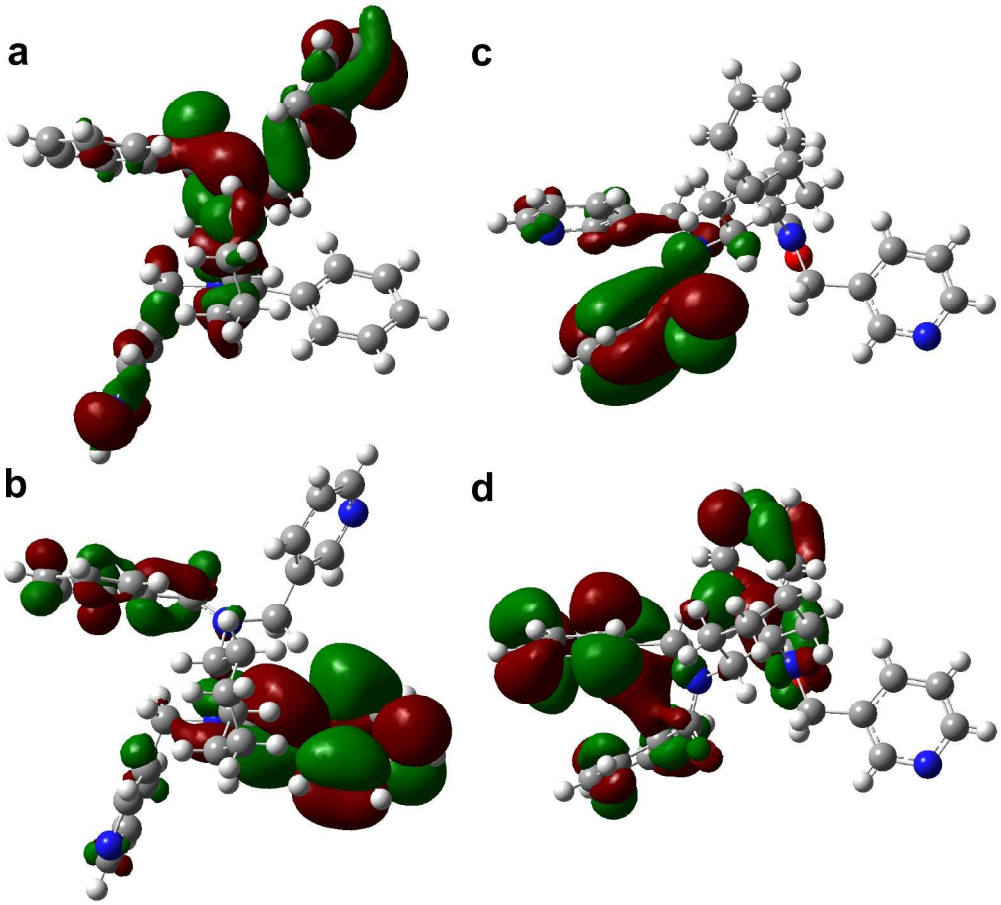


**Fig. 5** The contour plots of the relevant HOMO (a, c) and LUMO (b, d) for optimization models of the two configurations of (1*R*,2*R*)-3-bcpb in **1a** (**1b**) and **2a** (**2b**), respectively.
576x518mm (180 x 180 DPI)

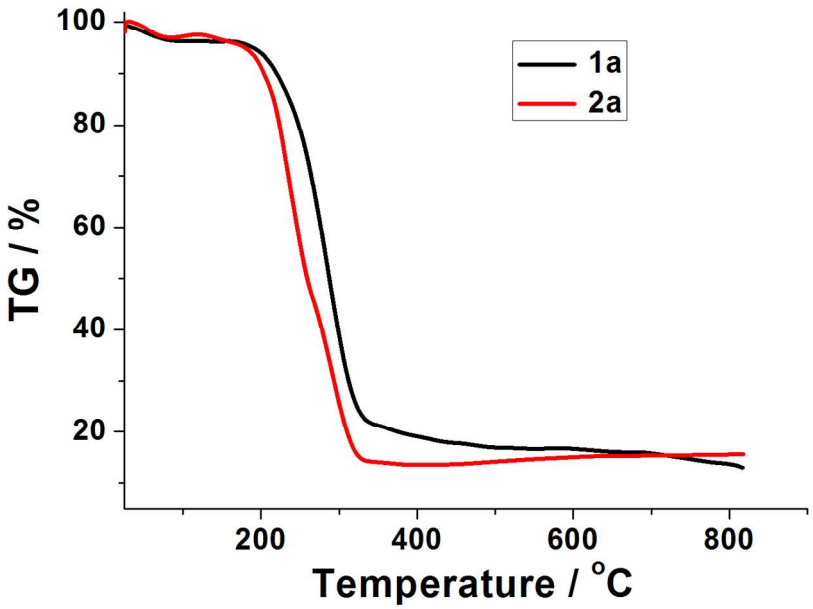


**Fig. 6** TG plots for **1a** and **2a**.
289x200mm (150 x 150 DPI)

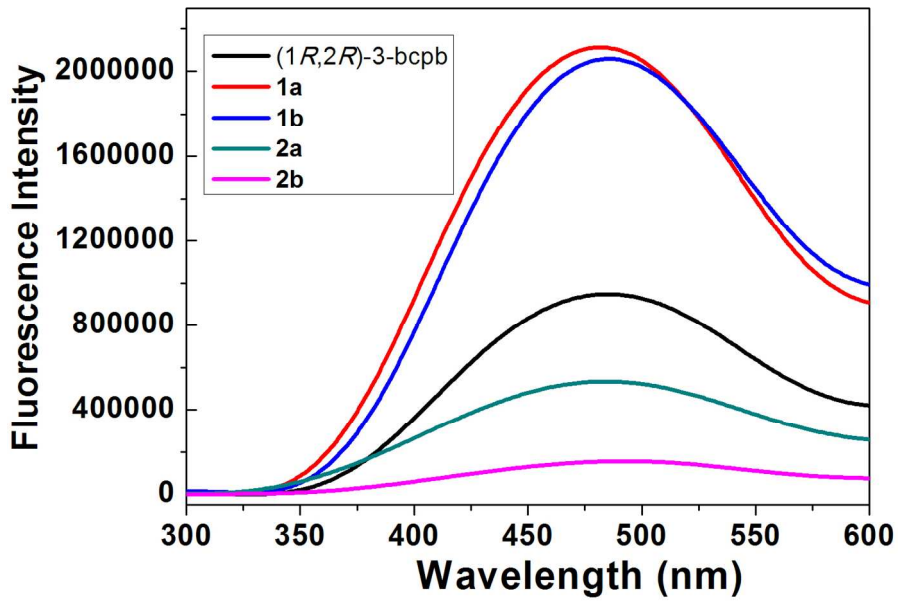


**Fig. 7** Luminescence spectra of (1*R*,2*R*)-3-bcpb and the four CCPs in the solid state at room temperature.
289x200mm (150 x 150 DPI)

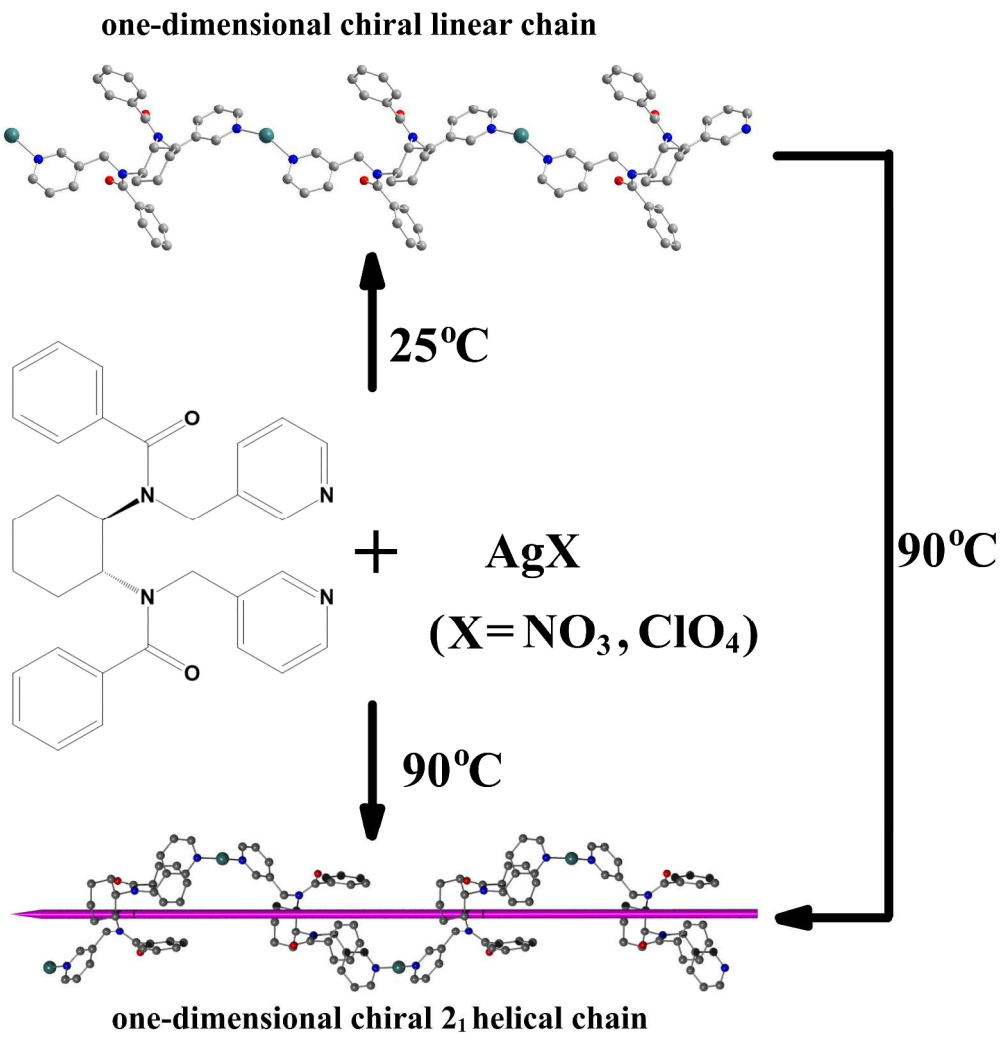


394x405mm (300 x 300 DPI)